JOURNAL OF MATERIALS SCIENCE 20 (1985) 2313–2322

The Ni_3Al–Ni_3Cr–Ni_3Ru section of the Ni–Cr–Al–Ru system

S. CHAKRAVORTY, H. HASHIM, D. R. F. WEST
Department of Metallurgy and Materials Science, Imperial College of Science and Technology, London SW7 2BP, UK

An investigation is reported of the 75 at% nickel section of the Ni–Cr–Al–Ru system at 1523 and 1273 K. Constitutional data obtained by electron probe microanalysis, X-ray diffraction and microscopical examination are presented as partial isothermal sections. At 1523 K, the major part of the section consists of γ phase, while the aluminium-rich region contains a γ' and a $\gamma + \gamma'$ region; the extent of the solid solution of chromium and ruthenium in γ' totals ~4 at%. The ruthenium-rich corner of the section shows a two-phase region consisting of γ + ruthenium-rich solid solution. At 1273 K the γ', $\gamma + \gamma'$ and γ + ruthenium regions increase in extent. The γ/γ' mismatch values in the equilibrated alloys studied lie in the range ~ −0.08 to −0.39%. Constitutional features of as-cast alloys are also reported.

1. Introduction

The platinum group metals (PGMs) have attracted interest in the field of nickel-based superalloy development and it has been shown that they act beneficially with respect to oxidation and corrosion resistance at high temperatures, without adversely affecting creep strength and other mechanical properties [1, 2]. The specific effects of platinum, rhodium, palladium and ruthenium have been reported and platinum enriched superalloys have been developed [1, 2]. Other research has shown beneficial effects of combined additions of PGMs and certain other elements such as yttrium, hafnium, or cerium [3]. In the area of coatings technology, the technique of depositing platinum onto nickel-based superalloys followed by treatments to produce an aluminium-rich layer is used to give improved protection in elevated temperature service as compared with conventional aluminide coatings [4, 5]. PGMs are also of interest in relation to M–Cr–Al–Y overlay coatings as additions aiming to improve the adherence between the scale and substrate under thermal cycling conditions [6].

In the context of these developments, there is a lack of information on the constitution of nickel-based ternary and higher-order systems containing PGMs. The work reported here is part or a research programme to obtain such constitutional information, relating particularly to the γ phase (nickel-rich solid solution) and the γ' phase (based on Ni_3Al). The programme covers the ternary systems Ni–Al–X where X is platinum, palladium or ruthenium. Concerning higher-order systems chromium is an important element and the Ni–Cr–Al ternary forms an excellent base because of its usefulness in representing important features of the γ/γ' relationships and also because the constitution of nickel-rich ternary alloys has been extensively studied. The present paper is concerned with the nickel-rich portion of the Ni–Cr–Al–Ru system. The role of ruthenium is an interesting subject for study since consideration of the relevant binary systems, particularly Ni–Ru and Ru–Al suggests some potentially advantageous alloying features in terms of solid solution and compound formation as discussed below; also the relative cost of ruthenium among the PGMs is an attractive feature. The present investigation is concerned with the 75 at% nickel section of the quaternary system which provides a good basis for exploring the γ/γ' equilibria.

2. Literature survey

Of the three ternary systems relevant to the nickel-rich corner of the quaternary system,

0022–2461/85 $03.00 + .12

experimental data are available for Ni–Al–Cr and Ni–Al–Ru; this information is briefly surveyed below together with comments on the likely form of the Ni–Cr–Ru system.

2.1. Ni–Al–Cr system

The complete system has been recently reviewed in detail by Merchant and Notis [7]. A number of investigations of isothermal sections include the 75 at% nickel line in the range 1423 to 1023 K and provide information on the γ/γ' relationships, [8–14]. There is extensive solubility of chromium in γ' increasing with decreasing temperature from 7.8 at% at 1473 K [10] to close to 20 at% at 1023 K [8].

2.2. Ni–Al–Ru system

The Ni–Ru system is of simple constitution showing a peritectic reaction: $L + Ru \rightarrow \gamma$ [15, 16]. The peritectic temperature has been reported as ~1763 K [17] or ~1823 K [18] and the peritectic liquid composition as 25 at% Ru [17] or ~28 at% Ru [18]. The solubility of ruthenium in γ at the peritectic temperature has been reported as ~41 at% [18], but recent work [19] supports the value of ~29.7 at% ruthenium found by Raub and Menzel [17]. The solubility of ruthenium in nickel decreases with temperature; at 900 K values of ~3 at% [17] and 7 at% [18] have been found. Lattice parameter data for γ have been determined [17, 18]. At the peritectic temperature, values of ~49 at% [17] and 47 at% [18] have been reported for the solubility of nickel in ruthenium; the solubility decreases to ~5 to 7 at% at 900 K. An investigation of rapidly solidified Ni–Ru alloys with 30 to 40 at% ruthenium has shown the existence of a metastable intermediate phase designated η with a tetragonal structure $a = 0.451\,06$ nm and $c = 0.362\,016$ nm [19].

The Ru–Al system contains a number of intermetallic compounds [15, 16] of which only RuAl is relevant to the present work. This phase is cubic, CsCl type; the lattice parameter is reported as 0.303 nm [20] or 0.295 nm [21]; the maximum extent of the single phase RuAl region is from ~49 to 58 at% aluminium at a temperature of ~1873 K. Liquid containing 30 at% aluminium undergoes a eutectic reaction at ~2193 K to form RuAl + Ru containing ~4 at% nickel.

The complete isothermal section of the Ni–Al–Ru system has been determined at 823 K using metallography and X-ray diffraction [22]; alloys were annealed at 1273 K for 700 h, followed by annealing at 823 K for 1400 h (for nickel-rich samples). In the region relevant to the present work, negligible solubility of ruthenium in Ni_3Al was found. NiAl was found to dissolve up to 5 at% ruthenium and RuAl up to 8 at% nickel. The three phase equilibria were found to be $\gamma + \gamma' + \beta$(NiAl); $\gamma + \beta$(NiAl) + RuAl; γ + RuAl + Ru. An investigation of the nickel-rich portion of the system (up to ~50 at% aluminium) at 1523 and 1273 K is being made by the present authors [23]. The solubility limit of the ternary γ field lies at ~14 at% aluminium, 23 at% ruthenium at 1523 K and ~14 at% aluminium, 13 at% ruthenium at 1273 K. The solubility of ruthenium in γ' at 1273 K is ~5 at%. The data available at present indicate very extensive mutual solubility between NiAl and RuAl with the possibility of complete mutual solubility at 1523 K; further work is in progress on this aspect. A three-phase equilibrium exists between γ, RuAl (containing ~43 at% aluminium, 32 at% ruthenium) and ruthenium-rich solid solution (Ru) containing ~3 at% aluminium and ~10 at% ruthenium. The 75 at% nickel line encounters the phases γ, γ', RuAl and (Ru).

2.3. Ni–Cr–Ru system

There appear to be no published investigations on the constitution of this ternary system. However, considering the binary systems, the Ni–Cr system is of the binary eutectic type [16, 24]. The eutectic is at 1618 K and liquid containing 54 at% chromium solidifies to form γ (containing 50 at% chromium) and chromium solid solution (containing 38 at% nickel). There is a substantial decrease in solid solubility with decreasing temperature; for example at 1273 K, γ contains ~45 at% chromium and the chromium solid solution contains ~5 at% nickel. An ordering reaction in the γ region is reported in a composition range based on Ni_2Cr.

The Cr–Ru system also shows a eutectic [16, 25]; this occurs at ~1883 K and at a liquid composition of 37.5 at% ruthenium to form chromium based solid solution (34 at% ruthenium) and ruthenium-based solid solution (52.5 at% chromium). These primary solid solutions show a marked decrease in solubility with decreasing temperature. At a temperature of ~1853 K, a sigma phase (~Cr_2Ru) [26] forms by a peritectoid between the primary solid solutions; other intermetallic compounds occur in the chromium-rich end of the system formed by solid state reactions.

As discussed above, the Ni–Ru system is of the peritectic type. On the basis of the binary diagram data the liquidus of the ternary system is likely to be of simple form, for example showing a ternary eutectic containing γ(f c c), chromium solid solution (b c c) and ruthenium solid solution (h c p). The major part of the system in the solid state is also expected to consist of equilibria involving these three solid solutions; near the Cr–Ru side of the system, equilibria involving the intermetallic compounds will be encountered. From the standpoint of the present work, only the γ solid solution region is directly relevant. Work is in progress to explore the constitution of the Ni–Cr–Ru system at 1523 and 1273 K [23].

3. Experimental procedure

On the basis of information deduced from the binary and ternary systems, it was possible to explore effectively the γ/γ' relationships with a very small number of alloys. A total of 4 quaternary alloys was prepared (Table I) using metals of purity nickel (99.99%), chromium (~99.9%), aluminium (~99.99%), ruthenium (~99.9%). Ingots of ~20 g weight were made by argon arc melting, several remelts being made to aid homogeneity. The melting losses were ~1.1 to 1.5%, which is unexpectedly larger than those typically found in the production of other model-nickel-based alloys [27]. The nickel contents of the alloys were found to be on the slightly nickel-rich side of the 75 at% nickel plane; the average nickel content from the data in Table I was 75.9 at%.

Portions of the ingots were cut for the examination of the as-cast state. The remaining portions of the ingots were sealed in silica tube under vacuum with a partial pressure of argon. Annealing was carried out at 1523 ± 5 K for 1 week followed by iced water quenching; after this treatment portions of the ingots were further annealed at 1273 ± 5 K for 2 weeks and iced water quenched. The 1523 K treatment did not completely remove coring from the as-cast structures; however, concentration gradients were not detected in the phases after annealing, indicating local equilibrium exists.

Microstructural studies were made using light microscopy, scanning electron microscopy (SEM) and transmission electron microscopy using extraction replicas.

Electron probe microanalysis (EPMA) to obtain tie-line and tie-triangle data was carried out using a JEOL JSM 35CF instrument with LINK system ZAF4 software; the relative error of the composition analysis was typically up to ~ ± 1% of the individual elements.

X-ray diffractometer examination was carried out on polished bulk samples using CuKα radiation, a graphite monochromator and a specimen spinner; the determination of lattice spacings was estimated to have an accuracy of ~ ± 0.2%.

4. Results and discussion

Data concerning phase compositions, lattice parameters and hardness are shown in Tables I and II. Figs. 1a to f show schematically the nickel-rich corner of the quaternary system. Liquidus projections for the ternary systems have been used as a basis for suggesting a possible form of the quaternary liquidus; this suggestion postulates an invariant reaction liquid $\rightarrow \gamma + \beta +$ chromium + ruthenium, although this equilibrium is not encountered in the composition range of the present work. Possible forms of the γ and γ' regions at 1523 K are also indicated.

4.1. Isothermal sections (Figs. 2a, b)

In constructing these isothermal sections at 75 at% nickel the $\gamma + \gamma'$ have been taken mainly from the work of Taylor and Floyd [8] for the Ni–Cr–Al system and the work of Chakravorty and West [23] for the Ni–Ru–Al and Ni–Cr–Ru systems.

At 1523 K the major part of the section consists of the γ phase. In the $Ni_{75}Al_{25}$ corner the γ' phase extends to ~2 at% ruthenium and chromium. The boundaries of the $\gamma + \gamma'$ region cannot be accurately located because the tie line compositions do not lie in the section (see Table II). In the equilibrated alloys, the γ compositions are nickel-rich with respect to the average alloy composition, lying between 75.6 and 77.3 at% nickel, while the γ' is relatively nickel-poor, lying in the range 74.7 to 76.0 at% nickel. The ruthenium-rich corner of the section contains a two-phase region of γ + ruthenium-based solid solution (Ru). With decreasing temperature to 1273 K, there is a marked increase in the extent of the γ', $\gamma + \gamma'$ regions associated with a reduction in the γ field; the γ + Ru region is also expanded (Fig. 2b).

It should be noted that alloys 1 and 2 located in the single phase γ region at 1523 K are shown by X-ray diffraction to contain some γ'; the latter forms during quenching from the annealing temperature as discussed in Subsection 4.3.

TABLE I Alloy compositions, hardness, lattice parameter and γ/γ' mismatch data

Alloy no.	Nominal alloy composition (at %)				Hardness (Hv)			Phases present and their structure with lattice parameter in nm						γ/γ' mismatch (%)		
	Ni	Cr	Al	Ru	as-cast	1523 K	1273 K	γ f c c			γ' (based on Ni_3Al) f c c			as-cast	1523 K	1273 K
								as-cast	1523 K	1273 K	as-cast	1523 K	1273 K			
1	75	6.25	16.25	2.5	237	232	218	0.3575*	0.3562 [0.3564]	0.3565 [0.3561]	0.3567†	0.3548‡	0.3552 [0.3560]	−0.22	−0.39	−0.36
2	75	2.5	16.25	6.25	229	223	211	0.3581*	0.3586 [0.3571]	0.3577 [0.3569]	0.3576†	0.3578‡	0.3574 [0.3570]	−0.14	−0.22	−0.08
3§	75	2.5	20.0	2.5	228	198	155	0.3569*	0.3572 [0.3567]	0.3571 [0.3568]	0.3565†	0.3569 [0.3568]	0.3569 [0.3565]	−0.11	−0.14	
4	75	6.25	3.25	15.5	199	176	186	0.3584*	0.3586 [0.3578]	0.3588 [0.3578]	0.3594†			+0.28		

*Primary phase in the as-cast condition.
† γ': lattice parameter after slow cooling.
‡ γ'' lattice parameter after quenching.
§Also NiAl (β) present in the as-cast condition. CsCl type b c c structure, $a = 0.2873$ nm.
The figures in square parentheses represent the calculated lattice parameter of respective γ and γ'.

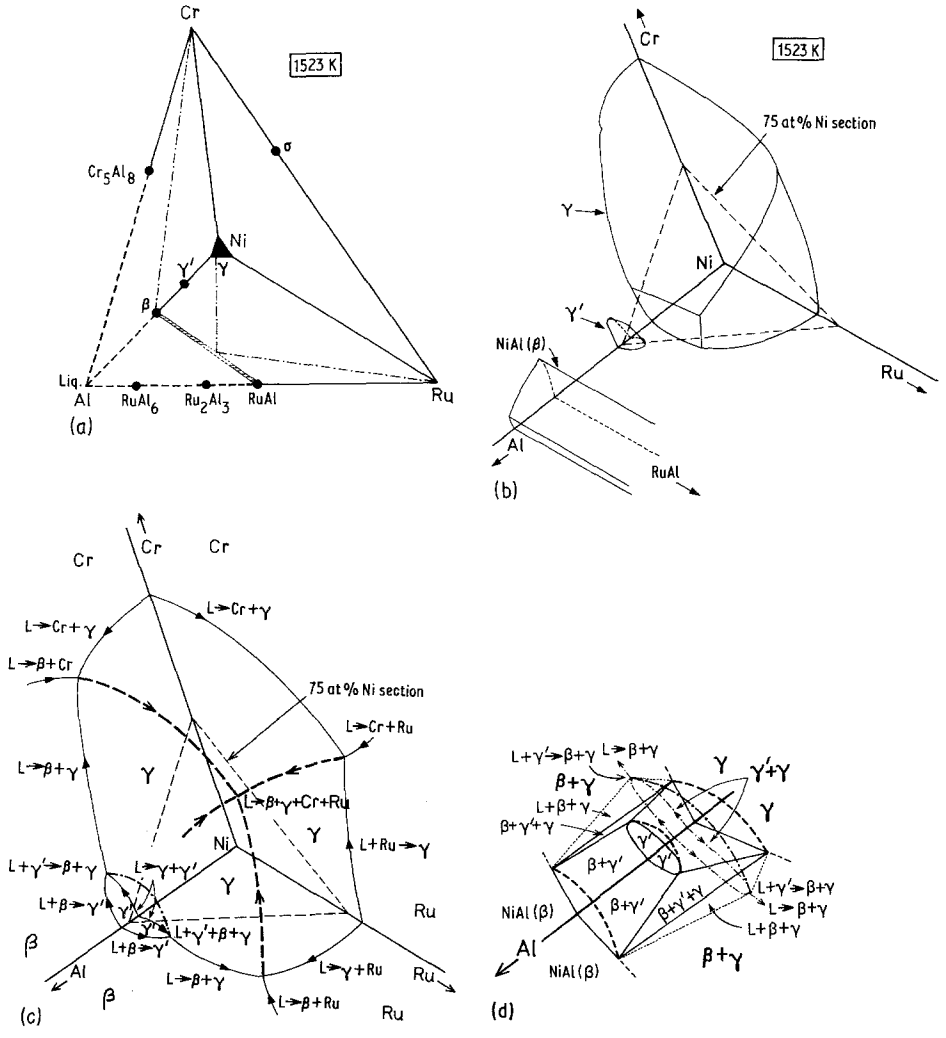

Figure 1 (a) Schematic representation of isothermal section of the Ni–Cr–Al–Ru system at 1523 K showing the phases present, based on data for the constituent binary and ternary systems [7, 8, 10, 15–17, 20, 23–25]. Equilibria are only indicated for the nickel-rich portion. The full extent of the single phase regions is not shown; however, it is assumed that NiAl (β) and RuAl show a complete series of solid solutions at 1523 K. The 3-phase tie triangle for γ, γ' and β is not shown, since with this method of representation, it is virtually coincident with the NiAl edge of the tetrahedron. Tie triangles for γ, β and ruthenium and γ, β and chromium are shown by –·–·–·–. (b) Schematic representation showing the approximate forms of the single phase γ, γ' and NiAl (β) regions at 1523 K in the Ni–Al–Cr, Ni–Al–Ru and Ni–Cr–Ru systems. Complete mutual solubility between NiAl and RuAl is assumed, but not entirely shown. (c) Schematic representation of the liquidus projections for the Ni–Al–Cr, Ni–Al–Ru and Ni–Cr–Ru systems. The liquidus data for the Ni–Al–Cr system are taken from refs. [7, 8, 10]. The data for Ni–Cr–Ru and Ni–Al–Ru are speculative and involve various assumptions including complete mutual solubility of NiAl and RuAl [23]. It is also assumed that the invariant reactions $L + \gamma' \rightarrow \beta + \gamma$ in the Ni–Cr–Al and Ni–Al–Ru systems are connected by a reaction curve in the quaternary system –·–·–·–; no arrow is shown on this projected curve since the reaction temperatures are not known. It is assumed that the quaternary system liquidus 4-phase reaction curves (– – –) lead to one invariant eutectic $L \rightarrow \beta + \gamma + Cr + Ru$ (β = NiAl/RuAl.). (d) The relationship between the above reaction curve and the solid state regions is shown. In the ternary systems, the invariant planes are represented in terms of the $\beta + \gamma + \gamma'$ and $L + \beta + \gamma$ tie triangles. – – – represents boundaries for β, γ' and γ projections in the quaternary system; –·–·–·– invariant reaction curve for liquid; –·–·–·– corresponding liquidus curves for ternary systems; --------- parts of $L + \beta + \gamma$ tie triangles in the ternary systems at the invariant temperature. The origins of the 4 three-phase eutectics in the β, γ, chromium, ruthenium tetrahedron are shown in (e). (f) Isothermal sections of the constituent ternary systems at 1523 K. The Ni–Cr–Al data are based on refs. [7, 8, 10]. The Ni–Al–Ru and Ni–Cr–Ru sections are based on ref. [23] and are subject to further experimental evidence. In the Ni–Cr–Ru system, there is evidence of an invariant solid state reaction $Ru + Cr \rightarrow \gamma + \sigma$ [23]. The Al–Ru–Cr system is speculative being based only on binary diagram data. Tie triangles are shown by –·–·–·–. Details of regions in the aluminium-rich corners of the sections are not shown.

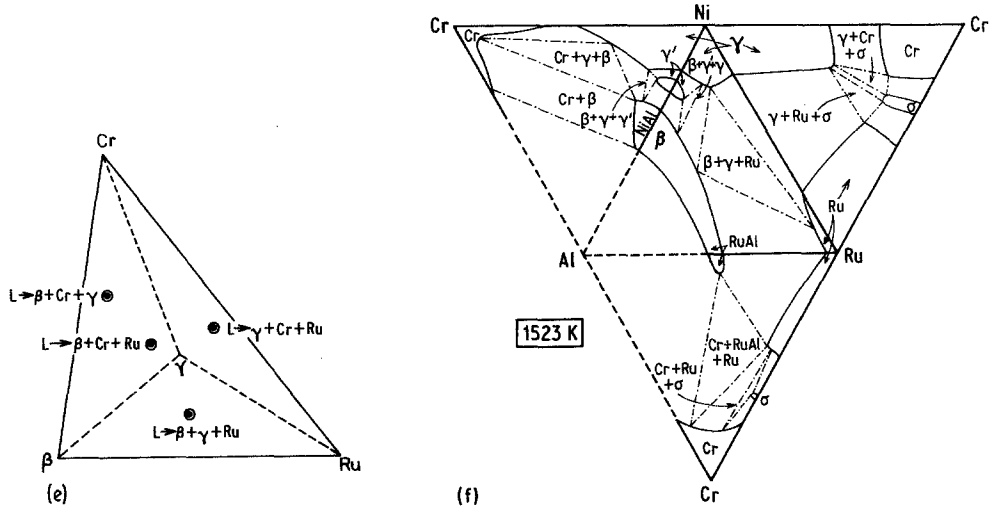

Figure 1 Continued

4.2. Lattice parameter data

Lattice parameter data for the γ and γ' phases are shown in Table I, together with γ and γ' mismatch data in the heat-treated alloys; the mismatch values are small and negative (in the range ~ -0.08 to -0.39%). Alloy 4 in the as-cast state shows a small positive mismatch value.

Values of γ and γ' lattice parameters were calculated using atomic diameter data [28]. γ and γ' parameters for binary Ni–Al alloys were taken as the basis with aluminium contents corresponding to the analysis data for Ni–Al–Cr–Ru γ and γ' (Table II). The agreement between measured and calculated data was typically within $\sim \pm 0.1$–0.4%. However, the limitation of the calculation procedure to the quaternary alloys is shown by the fact that applying it to binary Ni–Ru alloys using the lattice parameter of pure nickel as the basis gives significant differences between calculation and measurement; Vegard's law is not followed for the Ni–Ru solid solution [17].

4.3. Microstructure

All of the alloys in the as-cast state contained primary γ dendrites; etching revealed the structure in alloys 1, 2 and 3, but in the ruthenium-rich alloy 4, back-scattered electron imaging was required to show the features. The interdendritic

TABLE II Alloy compositions and phase compositions determined by EPMA

Alloy no.	Alloy composition determined by EPMA in at % Ni–Cr–Al–Ru	Sample treatment	Phases present	Phase composition determined by EPMA in at % Ni–Cr–Al–Ru	
				γ	γ'
	76.1–6.6–14.6–2.7	as-cast	$\gamma + (\gamma')$	78.2–6.3–12.7–2.8*	†
1	76.3–6.2–14.8–2.7	1523 K	$\gamma + (\gamma')$	76.3–6.2–14.8–2.7	†
	76.2–6.5–14.5–2.8	1273 K	$\gamma + \gamma'$	77.3–7.2–12.5–3.0	76.0–5.8–16.2–2.0
	75.8–2.5–14.3–7.4	as-cast	$\gamma + (\gamma')$	76.9–2.5–13.2–7.4*	†
2	76.0–2.5–14.9–6.6	1523 K	$\gamma + (\gamma')$	76.0–2.5–14.9–6.6	†
	76.2–2.6–14.5–6.7	1273 K	$\gamma + \gamma'$	76.5–2.7–14.0–6.8	76.0–2.4–16.6–5.0
	75.9–2.5–18.7–2.9	as-cast	$\gamma + \gamma' +$ ‡	77.8–2.5–16.6–3.1*	75.5–2.7–19.1–2.7
3‡	76.1–2.5–18.7–2.7	1523 K	$\gamma + \gamma'$	76.9–2.7–17.6–2.8	74.7–1.8–21.6–1.9
	75.7–2.6–18.9–2.8	1273 K	$\gamma + \gamma'$	76.8–2.9–16.9–3.4	75.6–2.4–19.5–2.5
	75.3–6.8–2.3–15.6	as-cast	$\gamma + (\gamma')$	77.8–6.8–2.3–13.1*	†
4	75.6–6.9–2.1–15.4	1523 K	γ	75.6–6.9–2.1–15.4	
	75.6–6.7–2.2–15.5	1273 K	γ	75.6–6.7–2.2–15.5	

* Primary phase in the as-cast structure; compositions correspond to central regions of dendrites.
† γ' precipitated during quenching/cooling. (γ') also indicates this.
‡ Nickel-rich β (based on NiAl) phase present in the as-cast state. Composition: 63.2 Ni–1.8 Cr–29.4 Al–5.6 Ru (at %).

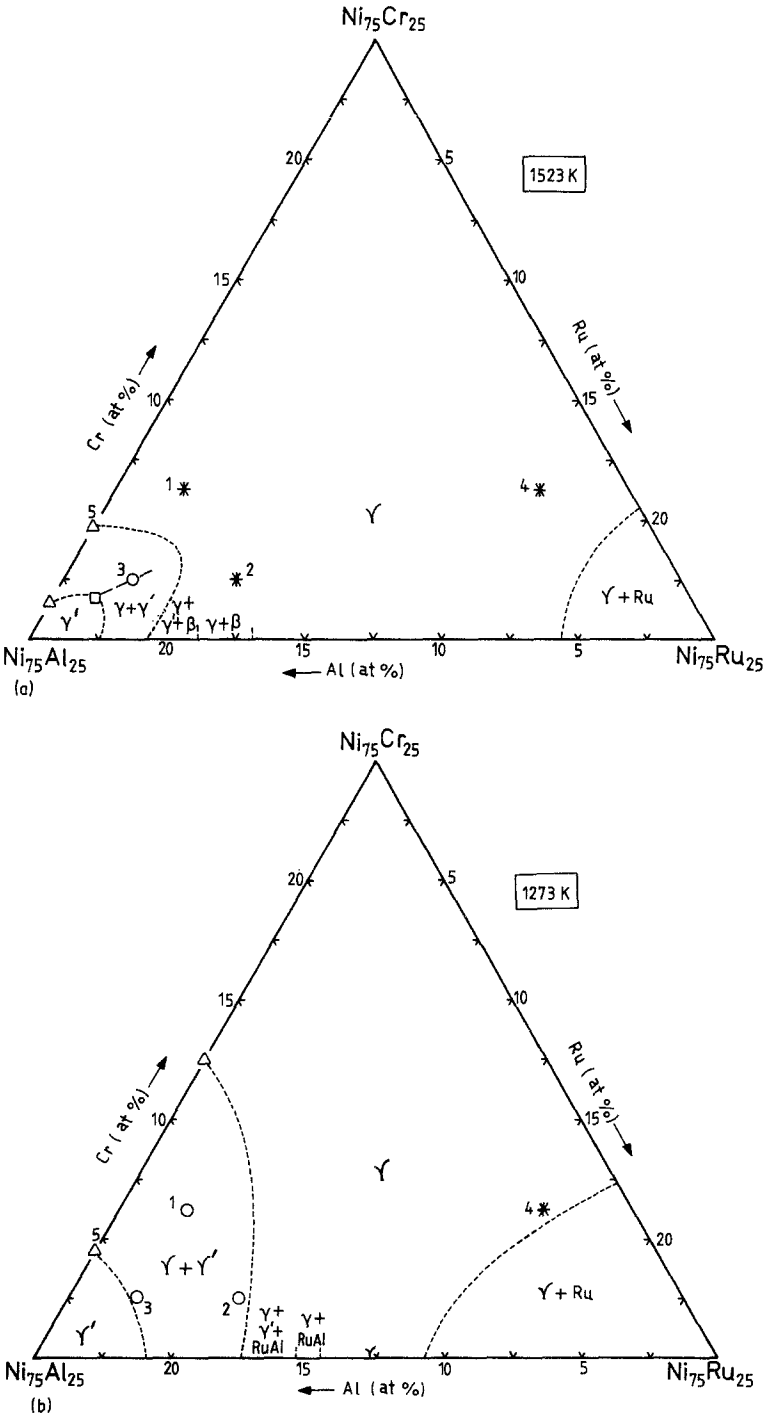

Figure 2 Partial isothermal section of the Ni–Cr–Al–Ru system at a nickel content of 75 at%. (a) 1523 K. (b) 1273 K. △ represent data for the Ni–Al–Cr ternary system and are from refs. [8, 10]. Experimental data on the Ni–Ru–Al and the Ni–Cr–Ru ternary systems are lacking. The boundaries shown are only estimated taking into account current work [23] and binary diagram data to indicate the types of equilibrium to be expected. The only phase composition data point included in Fig. 2a is of alloy 3, lying close to the 75 at% nickel section, i.e. within ~ ± 0.5 at%. In all other cases, the composition lies much above 75 at% nickel and interpolated phase boundaries are drawn close to appropriate phase compositions. Equilibrium involving β (NiAl), RuAl, γ and γ' have not been explored between the $\gamma + \gamma'$ and γ regions near the $Ni_{75}Al_{25}$–$Ni_{75}Ru_{25}$ section. All alloy compositions shown are nominal. □ phase composition by EPMA; -------- interpolated phase boundary; – – – – tie lines determined by EPMA; △ data from previous work; * single phase alloy; ○ composition of 2-phase alloy.

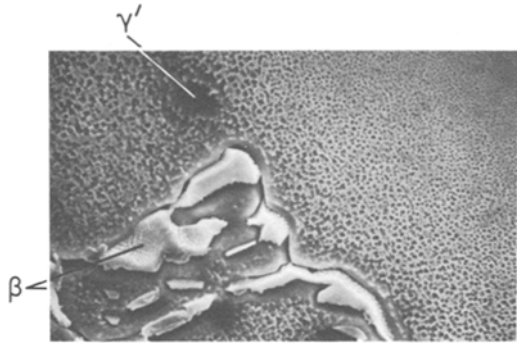

Figure 3 Alloy 3. Ni–2.5Cr–20Al–2.5Ru (at %). As cast. White β (NiAl) in aluminium-rich interdendritic region. Fine γ' cuboids, have precipitated in γ (grey) dendrites; the cuboid size decreases towards the centre of the dendrite. Some larger γ' regions (dark) are also present in and near the interdendritic region. SEM, etched $FeCl_3$/ethanol, × 3500.

regions in alloys 1, 2 and 4 showed areas richer in aluminium than the dendrites; these may be γ, enriched by segregation or may contain γ' phase. Alloy 3 showed particles of β and γ' in the interdendritic regions (Fig. 3); this is consistent with the liquid undergoing the $L \rightarrow \beta + \gamma$ reaction during solidification and the behaviour appears similar to that of a Ni–2.5Cr–20Al–2.5Mo alloy [14]. Fig. 3 also illustrates the solid state precipitation of γ' within the γ dendrites; the particles of γ' were larger in the outer regions of the dendrites, as a result of aluminium segregation giving a higher γ' solvus. All of the alloys (except alloy 4 in the annealed state) were shown by X-ray diffraction to contain γ' and this is attributed either wholly or mainly to solid state precipitation.

Structures of the alloys annealed for 2 weeks at 1273 K and for 1 week at 1523 K are illustrated in Figs. 4 to 7. The annealed alloys showed some coring effects; for example, the precipitate free

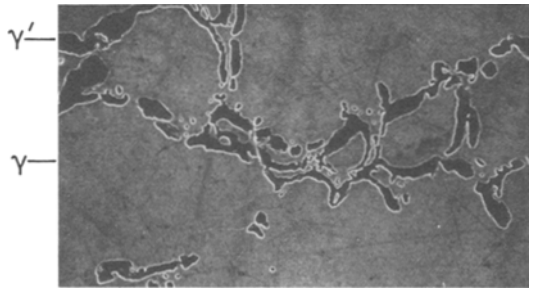

Figure 4 Alloy 3, Ni–2.5Cr–20Al–2.5Ru (at %). Annealed for 1 week at 1523 K, γ' (dark) in γ (grey) matrix. SEM, etched $FeCl_3$/ethanol, × 500.

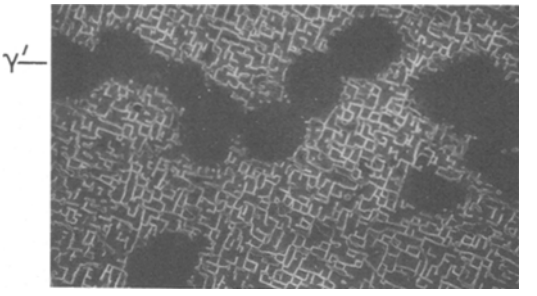

Figure 5 Alloy 3. Ni–2.5Cr–20Al–2.5Ru (at %). Annealed at 1523 K for 1 week + 1273 K for 2 weeks. Large γ' phase particles (dark) are retained from 1523 K. The remainder of the structure consists of a network of γ (light) surrounding precipitated γ' particles in the form of cuboids or "aggregated" cuboids. SEM, etched $FeCl_3$/ethanol, × 1000.

regions in Fig. 7. Also, in the $\gamma + \gamma'$ structure of alloy 3 annealed at 1523 K (Fig. 4), the irregular distribution of γ' is likely to be associated with higher aluminium contents remaining in the original interdendritic regions.

Figs. 5 to 7 show the precipitate dispersions produced by annealing for 2 weeks at 1273 K following annealing for 1 week at 1523 K. The sequence of alloys 2, 1 and 3 shows increasing proportions of precipitated γ', as anticipated from the positions of the alloy compositions relative to the boundaries of the $\gamma + \gamma'$ region (Figs. 2a, b). The main precipitation process occurs throughout the grains with the development of a raft-like morphology lying parallel to ⟨1 0 0⟩ [29–31]. Alloys 1 and 2 which were single phase γ at 1523 K show some grain boundary precipitation of γ', e.g. Fig. 7. Alloy 3 consisted of $\gamma + \gamma'$ at 1523 K and regions of γ' formed at this temperature are also seen after annealing at 1273 K (Fig. 5). In alloy 2 which contains only ~ 15 vol %

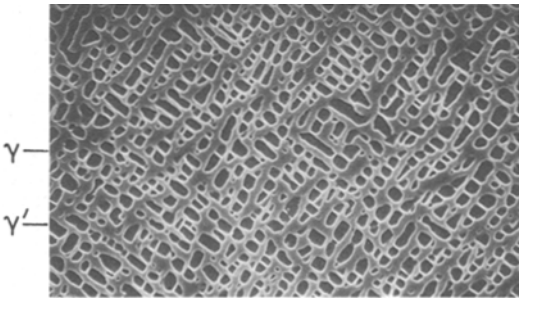

Figure 6 Alloy 1, Ni–6.25Cr–16.25Al–2.5Ru (at %). Annealed at 1523 K for 1 week + 1273 K for 2 weeks. Raft-like morphology of γ' (dark) in γ (grey) matrix. SEM; etched $FeCl_3$/ethanol, × 2000.

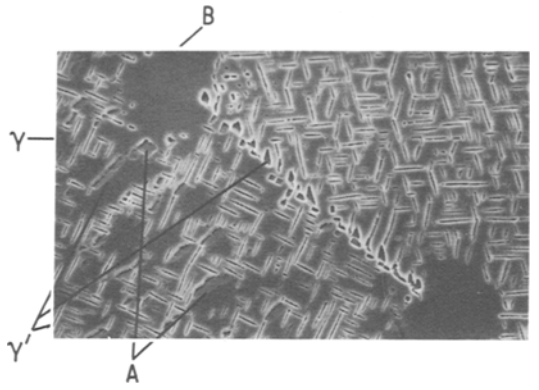

Figure 7. Alloy 2. Ni–2.5Cr–16.25Al–6.25Ru (at%). Annealed at 1523 K for 1 week + 1273 K for 2 weeks. Precipitates of γ' at γ grain boundaries and within γ grains; γ' within the grains is of plate-like morphology; the grain on the left-hand side of the micrograph has (1 0 0) close to the specimen surface; plate variants lying nearly parallel to the surface have been etched away leaving grey areas (e.g. at A). Regions free of γ' (e.g. B) are attributed to coring effects not removed by the annealing treatment. SEM, etched $FeCl_3$/ethanol, × 1000.

of γ' the precipitate takes the forms of plates typically of high length/width ratio (Fig. 7). The plate length ranges from ~1 to 12 μm and the width is ~0.5 μm; there is some tapering towards the plate extremities. Alloy 1 contains approximately equal proportions of γ and γ' (Fig. 6). The γ' rafts are of a rod-like nature formed by the joining together of cuboids; the raft length ranges from 1 to 7 μm and the width from 0.5 to 2 μm. In alloy 3, in addition to areas of γ' retained from annealing at 1523 K the structure is mainly a γ/γ' mixture in the form of a network of γ surrounding γ' particles (~85 vol% γ') (Fig. 5). Cuboid shaped γ' particles range from ~1 to 6 μm in size and some γ'-cuboids have aggregated into complex shapes.

Observations of replicas from alloys 1 and 2 quenched from 1523 K showed evidence of fine γ' particles (of the order of 100 nm or less in size); these formed during the quench from 1523 K.

4.4. Hardness

Considering the 1523 and 1273 K annealed states, alloys 1, 2 and 3 all contain γ and γ' taking into account the X-ray diffraction data and replica studies. However, a detailed correlation of the hardness with the structural features cannot be made in view of the lack of information on the fine γ'-dispersions produced during quenching.

An indication of the hardness level of γ' is provided by the value of 155 HV for alloy 3 quenched from 1273 K which consists predominantly of this phase. This value is comparable with that of a single phase γ' alloy in the Ni–Cr–Al–Mo system (namely ~160 HV) [14]. The hardness values of alloys 1 and 2, quenched from 1523 and 1273 K and of alloy 3 quenched from 1523 K lie within the range ~200 to 230 HV, and it can be inferred that γ' formed on quenching makes a significant contribution to hardness. In alloy 4 after annealing no γ' was detected and the solid solution effect of ruthenium is a major factor in producing the hardness level of ~180 HV.

All the as-cast alloys contain some γ'; the particle size was large enough to detect by scanning electron microscopy only in alloy 3 (Fig. 3). The hardness levels, lying in the range ~200 to 240 HV, are consistent with a dispersion hardening effect from γ'.

5. Summary and conclusions

The 75 at% nickel section of the Ni–Cr–Al–Ru system contains the γ and γ' phases and ruthenium-rich solid solution. In the γ' phase the solubility of chromium and ruthenium totals ~4 at% at 1523 K. The section consists predominantly of a single phase γ region at 1523 K, but the range of the γ region decreases at 1273 K by the increase in extent of the γ', $\gamma + \gamma'$ and γ + Ru regions. γ/γ' mismatch values are low and negative. Prolonged annealing at 1273 K gives rise to raft-like dispersions of γ' precipitate.

Acknowledgments

The authors acknowledge with thanks the support of SERC and the provision of ruthenium by Johnson Matthey Research Centre.

Note added to proof

Recent results obtained by the authors for the Ni–Al–Ru system [23] show that NiAl and RuAl do not exhibit complete mutual solubility at 1523 K as is assumed in Fig. 1. From the information now available, it seems unlikely that such solid solubility exists even at some higher temperature; in the absence of complete mutual solubility modification will be needed to the scheme of reactions shown in Fig. 1c.

References

1. C. W. CORTI, D. R. COUPLAND and G. L. SELMAN, *Platinum Met. Rev.* **24** (1) (1980) 2.

2. *Idem*, in Proceedings of the Conference on Behaviour of High Temperature Alloys in Aggressive Environments (1979), Petten.
3. A. S. DARLING and I. R. McLEAN, British Patent JX/5282/02, 50597/77.
4. R. G. WING and I. R. McGILL, *Platinum Met. Rev.* **25** (3) (1981) 2.
5. M. R. JACKSON and J. R. RAIRDEN, *Met. Trans.* **8A** (11) (1977) 1697.
6. E. J. FELTEN, *Oxid. Met.* **10** (1976) 23.
7. S. M. MERCHANT and M. R. NOTIS, *Bull. Alloy Phase Diagrams* to be published.
8. A. TAYLOR and R. W. FLOYD, *J. Inst. Met.* **81** (1952–53) 451.
9. I. I. KORNILOV and R. S. MINTS, *Akad. Nauk. SSSR, Izvest, Sektora Fiz-khimi. Analiza. Obschchei i. Neorg. Khimii* **26** (1955) 62.
10. *Idem, Zhur. Neorg. Khimi* **3** (1958) 699.
11. N. DELANERULLE and L. L. SEIGLE, SUNY at Stony Brook (1983) unpublished.
12. D. C. TU, PhD thesis, SUNY at Stony Brook (1982).
13. B. B. ARGENT, C. W. HAWORTH and N. C. OFORKA, University of Sheffield, private communication (1984).
14. S. CHAKRAVORTY and D. R. F. WEST, *J. Mater. Sci.* **19** (1984) 3574.
15. R. P. ELLIOTT, "Constitution of Binary Alloys", 1st Supplement (McGraw Hill, New York, 1965) pp. 54, 667.
16. F. A. SHUNK, "Constitution of Binary Alloys", 2nd Supplement (McGraw Hill, New York, 1969) pp. 40, 273, 277, 551.
17. E. RAUB and D. MENZEL, *Z. Metallk.* **52** (1961) 831.
18. I. I. KORNILOV and K. P. MYASNIKOVA, *Izv. Akad. Nauk SSSR, Met i Gorn. Delo, 4 (1964) 159; Russ. Met. Mining* **4** (1964) 95.
19. N. I. VARICH and A. N. PETRUNINA, *Metally (Russ. Metall.)* **2** (1979) 90.
20. W. OBROWSKI, *Naturwissenschaften* **47** (1960) 14.
21. A. MAGNELI, L. E. EDSHAMMAR, T. DAGERHAMN and S. WESTMAN, Final Technical Report No. 1 on contract DA-91-591-EUC-3134 (AD 451442) (1964) p. 6.
22. V. F. TSURIKOV, E. M. SOKOLOVSKAYA and E. F. KAZAKOVA, *Vestnik Moskovskogo, Universiteta. Khimiya* **35** (5) (1980) 512.
23. S. CHAKRAVORTY and D. R. F. WEST, to be published.
24. M. HANSEN and K. ANDERKO, "Constitution of Binary Alloys", 2nd edn. (McGraw Hill, New York, 1958) p. 541.
25. A. K. SHURIN and G. P. DMITRIEVA, *Sb. Nauchn. Rabot Inst. Metallofiz., Akad. Nauk. Ukr. SSR* **18** (1964) 170.
26. R. M. WATERSTRAT and J. S. KASPER, *Trans. AIME* **209** (1957) 872.
27. S. CHAKRAVORTY and D. R. F. WEST, *Met. Sci.* **18** (1984) 207.
28. *Idem, ibid.* **17** (1983) 573.
29. J. K. TIEN and S. M. COPLEY, *Met. Trans.* **2A** (1971) 543.
30. J. K. TIEN and R. P. GAMBLE, *ibid.* **3** (1972) 2157.
31. R. A. MACKAY and L. J. EBERT, *Scripta Metall.* **17** (1983) 1217.

Received 21 May
and accepted 4 June 1984